Nondestructive high-resolution and absolute mass determination of single charged particles in a three-dimensional quadrupole trap

Stephan Schlemmer,[a] Jens Illemann, Stefan Wellert, and Dieter Gerlich[b]
University of Technology Chemnitz, Institute of Physics, 09107 Chemnitz, Germany

(Received 6 December 2000; accepted for publication 27 June 2001)

A method for the nondestructive high-resolution and absolute mass determination of charged particles is described. It is based on the detection of light scattered from a single particle in an electrodynamical three-dimensional quadrupole trap. From the amplitude modulation of this signal, the eigenfrequencies of the secular motion are determined with high precision. For 500 nm in diameter SiO_2 particles, having a mass of 130 fg ($\approx 10^{11}$ u), a resolution of 10^{-4} is achieved in a 10 s measurement. On a longer time scale, the 10^{-6} range can be accessed. Key features of the method such as reproducibility, long term stability, accuracy, and linearity are characterized in detail. The extension of the mass range of quadrupole traps from atomic masses to micrometer sized particles as well as potential applications are discussed. © *2001 American Institute of Physics.* [DOI: 10.1063/1.1397295]

I. INTRODUCTION

The most important characteristics in mass spectrometry are resolution, mass range, sensitivity, dynamic range, and temporal response. Depending on the application, other features, such as whether a method is destructive or nondestructive or whether the method can distinguish between two species of the same mass but different properties, e.g., structural isomers, can be also important. The mass range of commercial methods in mass spectrometry (MS) such as quadrupole mass spectrometry,[1] time-of-flight mass spectrometry[2,3] and also ion-cyclotron-resonance mass spectrometry[4] is limited by a maximum *M/Q* value of the charged particles under consideration. Even with highly charged particles such as ions from an electrospray ion source, absolute masses greater than 10^6 u (≈ 1 ag $= 10^{-21}$ kg) are hard to access. However, mass determination of particles heavier than a few attograms is an important task in many fields of science, involving aerosols, biological particles (large biomolecules up to whole cells), and nanoparticles.

In their pioneering work, Wuerker *et al.*[5] demonstrated the electrodynamical containment of micron sized charged particles in a three-dimensional quadrupole trap, which is often referred to as the Paul trap.[6] This confinement in an electrical alternating field in combination with an additional dc field, compensating the gravitational force, i.e., levitation, is known as the electrodynamical balance (EDB). It has been and is widely used for the determination of the charge to mass *(Q/M)* ratio of micron sized particles. Although very useful, this method is restricted to particles with small *Q/M* values because gravity has to be significant with respect to the trapping force in order for the compensation voltage to be a sensitive balance of the mass. The resolution of EDB is limited to the percent range by the limited precision in determining the mean position of the moving particle.

Already in the early applications of quadrupole traps[5] it has been realized that under adiabatic conditions, $\eta < 0.3$,[7] the particles mean motion is in good approximation harmonic and that the eigenfrequency is a direct measure for its charge to mass ratio. Based on this idea, Hars and Tass[8] recently described a method which makes use of the fact that the motion of the particles is composed of the secular motion in a pseudopotential (frequency ω) and of a rapid motion (frequency Ω) due to the driving field. Tuning the driving frequency to an integer multiple of the secular frequency gives rise to a standing star pattern of the trajectory. In principle, this measuring procedure can be used to determine the charge to mass ratio with a precision in the 10^{-3} range. However, one has to make sure for this method that the scattered light intensity has to be sufficiently high to identify a complete image of the trajectory. Moreover, even for an eight branch star, deviations from adiabaticity spoil the accuracy of the method.

In the present study, we describe an alternative optical detection scheme to determine the eigenfrequency of the particles motion. Due to the precision of this frequency measurement, a resolution in the 10^{-5} range is reached routinely even with a rather simple setup. Experimental parameters are chosen to allow for a highly adiabatic secular motion, $\eta < 0.1$. The definition of the adiabaticity parameter η (Ref. 7) will be given below. In the limit, $\eta \to 0$, the eigenfrequency is exactly proportional to the charge to mass ratio. By changing the charge in a Millikan-type experiment, the absolute number of charges is determined and thus also the absolute mass of the particle. The accuracy of the method is discussed and the linearity is demonstrated for one particle the charge state of which was changed by a factor of three.

II. EXPERIMENT

A. Quadrupole trap—principle of operation

The general idea of the experiment is based on the fact that a charged particle in an alternating electrical quadrupolar

[a]Electronic mail: schlemmer@physik.tu-chemnitz.de
[b]Electronic mail: gerlich@physik.tu-chemnitz.de

field experiences harmonic restoring forces. As a result, the trajectory of the particles is dominated by eigenfrequencies for the radial and polar motion, ω_r and ω_z, the secular frequencies, which are proportional to its charge to mass ratio, Q/M. The theory of the quadrupole trap and the motion of a charged particle is very well established[1,9,10] and is not reviewed in this article. Here, we recall a few important equations needed for the analysis of the experiment and the range of applicability is discussed in some detail.

The equation of motion of a charged particle in a quadrupolar field,

$$\Phi=(U_0-V_0\cos(\Omega t))(2z^2-r^2)/2z_0^2, \tag{1}$$

where U_0 is the dc voltage applied in series with an ac voltage V_0 at an angular frequency Ω, is given as a special case of the Mathieu differential equation

$$d^2r/d\xi^2+(a_r-2q_r\cos(2\xi))r=0, \tag{2a}$$

and

$$d^2z/d\xi^2+(a_z-2q_z\cos(2\xi))z=0 \tag{2b}$$

with $\xi=\Omega t/2$ and

$$a_z=-2a_r=-8(Q/M)U_0/(z_0^2\Omega^2), \tag{3}$$

$$q_z=-2q_r=-4(Q/M)V_0/(z_0^2\Omega^2), \tag{4}$$

the so-called stability parameters.

The solutions are given by an infinite series of harmonic functions, each proportional to $e^{\pm i\beta r,z\Omega/2t}$, where β_r and β_z are related to $a_{r,z}$ and $q_{r,z}$. $\beta_{r,z}$ have to be real in order to stabley store the particle. For a given choice of $a_{r,z}$ and $q_{r,z}$, i.e., U_0 and V_0, the first harmonic component is dominant such that the two fundamental or secular frequencies, $\omega_{r,z}=\beta_{r,z}\Omega/2$, are governing the spectrum of the particles motion. By this means, the fundamental idea of the experiment that the particles charge to mass ratio can be determined by a frequency measurement is applicable. In the experiment, we choose for simplicity $a_z=0$ and $\eta=q_z<0.3$ such that the amplitude of the micromotions is very small compared to the amplitude of the secular motion. In this adiabatic limit, the motion can be well described by an effective harmonic potential, e.g., in z direction:

$$V_{\text{eff}}=\tfrac{1}{2}M\omega_z^2z^2. \tag{5}$$

In this case, the relation between the secular frequencies and the charge to mass ratio of the particle becomes very simple

$$\omega_z=|q_z|\Omega/(2\sqrt{2})=\sqrt{2}(Q/M)V_0/(z_0^2\Omega) \tag{6a}$$

and

$$\omega_z=2\omega_r. \tag{6b}$$

In return, when $\omega_{r,z}$ is determined in the experiment, and the parameters characteristic of the trap, i.e., Ω, z_0, and V_0 are known, Q/M can be determined by the simple expressions

$$Q/M=\sqrt{2}\omega_r\Omega z_0^2/V_0 \tag{7a}$$

and

$$Q/M=\frac{\sqrt{2}}{2}\omega_z\Omega z_0^2/V_0. \tag{7b}$$

Several remarks and precautions regarding the applicability of these two simple relations should be made. For that matter, the assumptions made for their derivation have to be recalled.

First, the field has been idealized as quadrupolar only [see Eq. (1)]. In this case, the eigenfrequency is independent of location and of amplitude. Such an ideal electrode arrangement can not be realized in practice. Even the Paul trap arrangement with hyperbolically shaped electrodes is imperfect due to the boundary conditions imposed by the finite extension of the electrodes. Therefore, the true potential Φ is composed of a series of multipole components[11,7] each of which satisfying the Laplace equation and which origins are at the center of the trap. Large efforts have been made in order to design a *real* trap where most of the multiple terms except the quadrupole term vanish due to a good choice of the design of the electrodes, i.e., its boundary conditions.[12] The boundary conditions for the present trap will be described and discussed in the following experimental section. Here, we would like to draw attention to the fact that higher order multipole terms contribute to the field only at larger amplitudes. Provided a typical amplitude of about $z/z_0=0.01$, the field of the octopole term, in practice, the next highest term following the quadrupole term, is only 4×10^{-4} of the quadrupole term even when assuming its coefficient to be unfavorably large, 100% that of the quadrupole. Therefore, we conclude that for most practical quadrupole trap geometries, it is easier to try to restrict the motion to small amplitudes than to avoid higher order multipole terms.

Second, in the Mathieu differential equation, no other forces than the electrical ones have been accounted for. Gravity,[5,13] drag due to gas friction,[14,15,13] or various other *external* forces such as light scattering or gradient forces[16] have been accounted for in more advanced treatments in the literature. An example for an *internal* force, related to the particle in an inhomogeneous field, is the dielectric force which becomes relevant for low charge, heavy particles.[17] For the present study, gravity has been compensated in most cases by an additional vertical dc field which will be described in the next section. However, the gravitational force or the additional field in case of compensation leads to a small systematic shift of the eigenfrequencies. Although very small, these aspects have to be borne in mind when discussing the accuracy of the method.

Third, the theoretical description treats the charged particle as a point mass and point charge. The numerous applications of the EDB show that this assumption is quite reasonable. However, forces which arise from the fact that the center of gravity and the center of charge may differ should be taken into account. For particles carrying only a few charges which are located on a spot of its surface, this effect increases with the size of the particle and it is reduced for a centrosymmetric particle when it is charged more evenly. In return, such forces can lead to a rotation of the particle and apparently to a more complex spectrum of motional frequencies which will be studied in future work.

Fourth, this derivation relies on the adiabaticity of the motion or the validity of the effective mechanical potential.

This holds only for conservative forces acting on the particle. However, the particle is subject to friction even at very low gas pressures. Therefore, the amplitude of the motion of the particle should be dampened to rest. Due to the statistical nature of the gas collisions (fluctuation–dissipation theorem) the average amplitude, $z_{\max}$, is derived from the temperature of the gas, i.e.,

$$\langle E\rangle=\langle V_{\text{eff}}\rangle+\langle E_{\text{kin}}\rangle=3kT \tag{8}$$

leading to

$$\tfrac{1}{2}M\omega_z^2\langle z_{\max}^2\rangle=kT/2. \tag{9}$$

Typical residual amplitudes are $z_{\max}\approx 50$ μm at 300 K. These amplitudes have to be small compared to the dimension of the trap, z_0, in order that forces due to higher order multipole terms do not play a role. In the present case, the ratio $z_{\max}/z_0=50$ μm/3.9 mm$=0.013$ is so small that frequency shifts due to anharmonicities can be neglected.

In summary, from these theoretical considerations, the following aspects for the design of the trap can be derived. For a very well reproducible *Q/M* determination, the field of the trap should be dominated by the quadrupole term. The driving voltages U_0 and V_0 and its angular frequency, Ω, have to be quite stable. Moreover, the electrode arrangement of the trap has to be mechanically and thermally stable. From a practical point of view, surface charges which give rise to additional potentials are equally important according to our experience and have to be considered, too.

B. Experimental setup

1. Trap design

The basic idea of the experiment is the continuous monitoring of a single trapped particle using the optical detection of the eigenfrequency of its motion. As has been already demonstrated more than 20 years ago, a single stored atomic ion can be observed by its laser induced fluorescence.[18] The scattering of light from a particle is another very universal phenomenon which is used in the present experimental setup.

In order to collect a large fraction of the scattered light, a wide viewing angle is one of the most important boundary conditions for the experimental setup. Figure 1 shows a schematic view of the full setup of the experiment. The very open design, 0.6 sr solid angle for viewing, does not allow for a closed electrode arrangement such as traditionally used for a Paul trap, consisting of two end caps and a ring electrode. The trap design used has been described in great detail[19] and here only a few key features will be given. Two conically shaped end caps which are separated 6.6 mm determine the symmetry axis, *polar* direction [perpendicular to the plane shown in Fig. 1(a)], of the trap. The ring electrode is replaced by eight rods which form a cage-like structure. The ac voltage for the driving field is applied to the cones only. Typical values are $V_0=750$ V (Ref. 20) and $\Omega/2\pi=500$ Hz. Details of the driving circuit are also given in Ref. 19. Pairs of the rods are electrically connected and used to control the *horizontal* and *vertical* position, *x* and *y* direction in Fig. 1(b), by applying a symmetrical dc voltage to opposing pairs. The quadrupole parameter, $z_0=5.50$ mm, which enters Eq. (7) has been determined using the ion optics simulation program SIMION.[21] The field parameter for the dc positioning has been determined as $E/(V\ m^{-1})=29.04\ \ U_{\text{dc}}/V$.

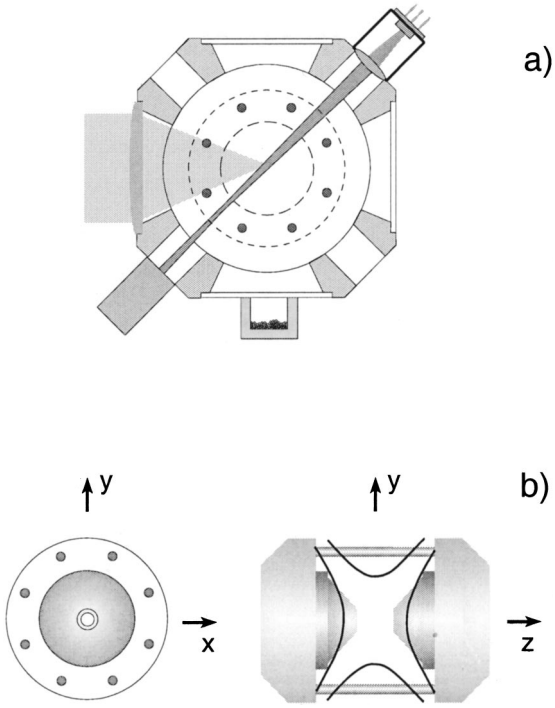

FIG. 1. Schematic cross sectional view of the central part of the experimental setup. (a) Housing with three-dimensional quadrupole trap (cut in the *x–y* plane), laser illumination of particle, and optical detection scheme in 45° forward direction is presented along with the particle injection from below. Instead of the rotationally symmetric ring electrode, eight rods enable a large viewing angle and additional horizontal (*x*) and vertical (*y*) positioning of the particle. For clarity, the electron gun, the gas inlet, and other tools are not shown. (b) Design of the trap electrodes. The eight steering rods and one conical end cap electrode are seen in the *x–y* plane (left-hand side). Both end cap electrodes and the bottom and top steering electrodes are shown in the *y–z* plane (right-hand side). In addition, the boundary conditions of the apparent quadupole term of the field expansion is given as a contour in the right-hand side graph.

The trap is mounted to a housing which serves as an electrical shield to possible outside stray fields and as a base for further attachment of equipment to the trap. This housing is mounted on a CF 100 flange such that it is located at the center of the UHV chamber of the experiment to make it accessible to other experimental tools.

As a collimated light source, a laser diode[22] at $\lambda=685$ nm with a maximum power of 50 mW has been used. The laser is mounted to the housing of the trap inside the vacuum in order to minimize any residual motion of the laser with respect to the center of the trap, see Fig. 1(a). A cross sectional area of the beam of 435 μm$\times$209 μm near the center of the trap is produced by using an aspherical lens (NA$=0.5$, f$=4.4$ mm). In the experiments shown here, a laser power of only a few mW gave sufficient scattered light signals. Corresponding power densities were only 30 kW/m^2. At the maximum power density of 1.4 MW/m^2, the corresponding light scattering force to the particle gives rise to an acceleration of about 1 m/s^2, i.e., 10% of the gravitational force, which can be used as an additional tool in future experiments. In general, also heating of the particle by light ab-

sorption is an interesting feature of the setup. By choice of the wavelength, it can be neglected in the present study.

Essential for the determination of the eigenfrequency is the modulation of the scattered light intensity by the particles trajectory. Therefore, the illumination of the particles has to be inhomogeneous. In the present setup, this is realized by the Gaussian beam waist of the collimated laser beam. Note that the beam waist and the amplitude of motion are of the same order of magnitude which leads to a large degree of signal modulation. The obvious advantage of this method is the collection of scattered light at all times as compared to a setup where, e.g., the particle is travelling in and out of the light. For the same reason, the signal contains all frequencies of motion and due to the nonlinear modulation sum frequencies as well as higher order harmonics are generated. Therefore, more than just the two secular frequencies usually appear in a spectrum.

2. Detection and signal processing

From the theory of light scattering from small particles, see, e.g., Ref. 23, it turns out that for spherical particles smaller than the wavelength of the light, radius $a<\lambda$, and a refractive index $n\geqslant 1$, most of the light is scattered in forward direction. In the present configuration, a large cone of acceptance for the detection of the scattered light has been chosen, see Fig. 1. The detector is an avalanche photodiode (APD)[24] which allows for the detection of light levels as low as pW. Fifty percent of the collected light is split off and directed to a conventional charge coupled device (CCD) cameras as a second detector for inspection and control purposes. The electrical signal of the APD is preamplified and filtered by a tenth order Butterworth analog filter whose corner frequency is set to 1/7 of the driving frequency to avoid aliasing. The resulting signal is recorded by an AD converter in a PC. As a time base for the experiment, the very stable oscillator of the driving frequency, Ω, is used. Each measurement is triggered by every sixth zero of this sinusoidal driving voltage. The spectrum contains 2048 points and is Fourier transformed for analysis. The measuring time is given by

$$T=2048\cdot 3/(\Omega/2\pi). \tag{10}$$

Typical values are in the range from 5–15 s. Correspondingly, the Nyquist frequency is given by $\omega_{\max}/2\pi = 1/6\Omega/2\pi$. As a result, the full spectrum is limited by $\beta_{\max}=1/3$ or $q_{\max}=\sqrt{2}/3\approx\frac{1}{2}$. Thus the eigenfrequencies recorded in these spectra always obey the adiabaticity limit.

3. Particles and their injection

A small UHV compatible loudspeaker is mounted below the trap and serves as storage for the particles prior to injection. It is filled with monodisperse SiO_2 particles which have a nominal diameter of 500 nm.[25] For injection, the membrane vibrates at about 1.5 kHz and ejects a swarm of particles into the trap. Acceleration to final velocities on the order of m/s can be expected at amplitudes of the membrane of about 100 μm. This corresponds to an initial kinetic energy in the keV range. Instead of using keV deceleration fields, gravity is used to slow down the particles since their flight height is about 10 cm. Therefore, the particle turns around near the center of the trap making trapping a likely event, see also Fig. 1(a). Other important tasks of the particle source are the deagglomeration of the particles and their charging. In the experiment, it turns out that the 500 nm particles trapped typically carry a few up to a few ten positive elementary charges.

4. Additional experimental tools

For the electron bombardment experiments, an electron gun[26] is pointing to the center of the trap through a hole in one of the end caps of the trap. Due to the one phase operation of the trap, the energy of the electrons is determined by the phase lack between the injection pulse and the ac driving field. This has been used to vary the energy and to observe differences in the yield and probability distribution of the number of secondary electrons. This process has been studied in some detail and first results will be published elsewhere.[27] Here, the gun serves only as a source of electrons for changing the charge state of the particle. Other open sides of the trap are used for leaking in gas (air, He, H_2; continuous wave and pulsed in operation) in order to study the frictional forces on the particle. Also, an oven containing condensable material is mounted at one port of the trap. The evaporation of C_{60} from the oven and its condensation to the particle has been used to demonstrate the *in situ* preparation and manipulation of a particle using the method described here.[27]

III. HIGH-RESOLUTION MEASUREMENT OF THE EIGENFREQUENCIES

The experiment starts with the injection of a particle under vacuum conditions. In most cases, the trajectory has initially an amplitude on a mm scale as observed by the CCD camera such that it occurs only as a dim filament. Using helium buffer gas at a pressure around 10^{-4} mbar, the motion of the particles is damped to its thermal amplitudes within a few tens of seconds. Since the laser is pointing mainly to the center of the trap, the trace on the screen appears much brighter. The vertical dc voltage is then used to compensate gravity such that the particle moves around the electrical center of the trap. In cases where more than one particle has been trapped, the particles end up in different positions along the vertical axis due to their different charge to mass ratio. Although a neighboring particle might not be seen easily, the Coulomb repulsion disturbs the motion of the one viewed. Then, the trap frequency is increased and the trapping potential becomes too shallow to trap all particles except the one with the largest charge to mass ratio. By this method, one makes sure to trap just a single particle at a time. Also, other methods for the selection of a particular particle can be chosen, e.g., the traditional way of mass selection in a quadrupole by adjusting $a_{r,z}$ and $q_{r,z}$ or resonant excitation of the secular frequency.

Figure 2(a) shows a typical result of a fast Fourier transform (FFT) of a single 10 s, 2048 points, measurement of

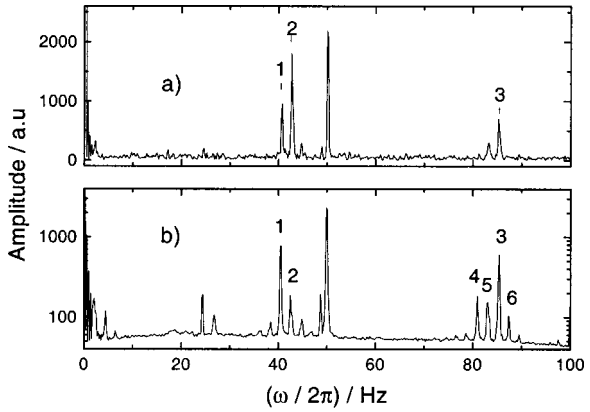

FIG. 2. Spectrum of the motional frequencies of a single trapped 500 nm SiO_2 particle obtained by a FFT of the scattered light signal. Operating conditions were $\Omega/2\pi=1193$ Hz and 2 $V_0=1673$ V (see Ref. 20). (a) Result from a single 10 s measurement and (b) an average over 500 measurements displayed in a semilogarithmic graph are shown. Besides the main eigenfrequencies of the motion of the particles in the quadrupole trap, $\omega_y/2\pi, \omega_x/2\pi$, and $\omega_z/2\pi$, denoted 1, 2, and 3, respectively, various combinations and higher harmonics thereof can be clearly identified. See Table I for the assignment of the peaks 1 to 6.

such a particle. Clearly seen are two frequency components close to 40 Hz, a peak at 50 Hz and a group of peaks close to 85 Hz. Besides the 50 Hz peak which is related to the pickup of electrical noise, the three most intense peaks have been identified as given in Table I. As it turns out by this measurement, not only are two fundamental frequencies ω_r and ω_z (denoted 3 in Fig. 2) present in the spectrum but the radial frequency splits into two components, ω_x and ω_y (denoted 1 and 2 in Fig. 2), which differ by as much as 5%. Such differences become easily detectable by the present high precision measurement. All three frequency components are present in the spectrum. This is due to the current choice of the direction of the laser with respect to the trap orientation, i.e., not pointing along one major axis of the trap. This arrangement is practical for the current functional tests but might be changed in future work to pick just one frequency for simplicity.

In order to assign the two radial frequencies to spatial directions, resonant enhancement of the amplitude of motion has been employed by applying a small ac voltage of varying frequency to vertical and horizontal pairs of rods. The assignment of ω_z is easy because due to theory it should be twice the radial frequency. However, in the vicinity, there are several other minor peaks which are due to various combinations and overtones of the three fundamental frequencies. For clarity, an average of 500 such measurements is displayed in a semilogarithmic plot in Fig. 2(b). During this time, no intentional changes of the charge of the particles or mass have been made such that the eigenfrequencies remain constant. Thus, the six most intense peaks are assigned as given in Table I.

The observed deviations could be attributed to a minor mechanical misalignment or displacement of the traps polar axis with respect to its x–y plane or a deformation of the circumference on which the eight rods are located to resemble the ring electrode of the Paul trap, see Fig. 1 and Ref. 8. Another reason may be the electrical fields due to the surface imperfections. Also, as discussed in the previous section, particle properties giving rise to additional forces, can be responsible for this splitting. In order to elucidate this point, the trap was operated with the polar axis horizontal (results shown here) and vertical. In the horizontal case, it turns out that $2\omega_x=\omega_z>2\omega_y$. In the other case, no splitting of ω_r was visible and $2\omega_r>\omega_z$ was found. Taking both results into consideration, it seems that the horizontal frequencies are increased while the vertical frequency is not affected. On the one hand, this might be correlated with particle properties, e.g., internal motion of the particle due to deviations from the point mass and point charge; on the other hand, additional surface charges, e.g., from charged dust on the lower electrode, and their corresponding field deviations could be responsible. Therefore, further more systematic experiments along these lines are necessary to clarify the reasons of this experimental finding.

A. Resolution

Upon identification of the particles eigenfrequencies, they can be followed over hours, days, or weeks in order to obtain relative mass or charge changes as a function of time. Due to the FFT procedure, the resolution of the method is limited by the measuring time T, i.e., $1/T$. Provided that there is no limitation to this time due to restrictions in data recording or its analysis, the product of the resolution $(1/T)$ and the temporal resolution of the experiment (T) when monitoring the mass as a function of time in a real experiment is constant. In the present setup and data acquisition system, the measuring time is however limited due to the fact that the sampling rate has to be fast enough to record the highest secular frequency desired, i.e., $1/6\ \Omega/2\pi$, and due to the limited number of channels in a record, i.e., $N=2048$ [see Eq. (10)].

The FFT signal has a line shape and is therefore distributed into several channels. Since in the present experiment there are no unresolved neighboring peaks, the peak position is known to a precision, what we call resolution, better than one channel. The peak position is determined by the maximum of the parabola which is given by the three neighboring points of maximum amplitude. Therefore, the *S/N* level en-

TABLE I. Assignment of the six most intense frequencies components given in the spectrum of Fig. 2(b).

Peak No.	1	2	3	4	5	6
Assignment	$\omega_y/2\pi$	$\omega_x/2\pi$	$\omega_z/2\pi$	$2\ \omega_y/2\pi$	$(\omega_x+\omega_y)/2\pi$	$(\omega_z+\omega_x-\omega_y)/2\pi$
Position/Hz	40.499	42.539	85.429	80.959	82.974	87.494

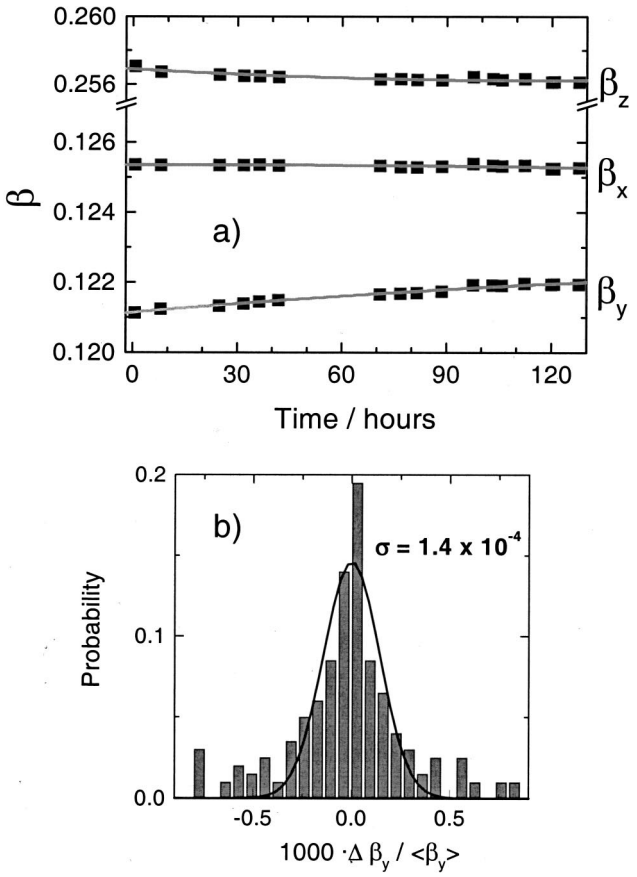

FIG. 3. Long term frequency measurements over a period of six days. (a) Long term stability: Temporal evolution of the three normalized fundamental eigenfrequencies, β_y, β_x, and β_z. Each point is the average of 100 individual measurements of 9.5 s duration. The spline fits indicate drifts on the 10 ppm/h level. (b) Reproducibility: Histogram of the probability determining the average frequency $\langle\beta_y\rangle$ for the first 200 individual measurements. A standard deviation of 1.4×10^{-4} for an individual 9.5 s measurement is in good agreement with the expected resolution.

ters the resolution as a second quantity when determining the position of the maximum of the signal amplitude in the frequency domain. This quantity increases as the measuring time is increased. Thus, the resolution of the experiment is increased with respect to the simple FFT considerations. In simulations, it has been found that the standard deviation in the frequency determination is given by $0.5/(T_1 S/N)$. At an eigenfrequency of 40 Hz, a measuring time of 10 s and a typical *S/N* of 10 this results in a resolution with a standard deviation of σ=0.005 Hz or relative to the peak position of 125 ppm.

B. Reproducibility

From a practical point of view the ultimate resolution is limited by the reproducibility and long term drifts of the experiment. In order to sort out different sources, long term measurements have been made. Figure 3 shows the result of a measurement with one particle over a period of six days. In Fig. 3(a), the three fundamental frequencies are plotted as a function of time. For the purpose of comparison, they are normalized to half the driving frequency, $\beta=2\omega/\Omega$, see Sec. II. Each point corresponds to the average of a hundred 9.5 s measurements at a total of about 2000 measurements. The scatter in the first 200 measurements of the vertical frequencies is plotted as a histogram in Fig. 3(b). This distribution has been fitted to a Gaussian with a standard deviation of 140 ppm. This value is in good agreement with the expectations for the present setup. Moreover, it shows that on an hour timescale, fluctuations and drifts are smaller than the resolution.

Our results can be compared to those of the electrodynamical balance.[28] The authors report a standard deviation of 1%–2% for the relative mass determination of particles 2.35 μm in diameter. This resolution has been largely improved by the more recent method developed by Hars and Tass.[8] Adjusting the driving frequency Ω such that the trajectory appears as a standing star pattern, an integer relation between the eigenfrequency, ω and Ω can be established. A resolution of about 10^{-3} has been reported. In summary, with the present experiment, the mass of a submicron particle is routinely determined with an improved precision of 10^{-4} in 10 s and up to a 10^{-5} level over a period of 1 h. This resolution is already sufficient to detect submonolayer changes in mass for the comparably large 500 nm particles. This makes the apparatus an interesting tool for surface science experiments. Further improvements will certainly lead to resolutions beyond the ppm range. Other advantages of the method reported here will be discussed next.

C. Long term stability

As seen in Fig. 3(a), the three eigenfrequencies show drifts of up to a percent during the six days of investigation. Note that the polar frequency, *z* direction, is dropping while the vertical frequency, *y* direction, is increasing by approximately the same amount. The horizontal frequency, *x* direction, shows the smallest drift (700 ppm over 140 h). Since changes in charge or mass lead to proportional changes in all three frequencies, see Eq. (6), the observed drifts are not related to changes in mass or charge. The same is true for the influence of the other quantities which enter Eq. (6), i.e., a change in z_0, V_0, or Ω. However, a careful analysis of the influence of the dc compensation field shows that its influence on the vertical and polar frequency is much stronger than on the horizontal frequency as observed in Fig. 3. Therefore, we assume a change in the vertical dc field on the order of a few ten V/m which corresponds to a change in the apparent voltage of less than a volt. As discussed before, these effects can also be due to changes in surface potentials. At this point, other sources for the drifts can not be excluded. However, in future experiments the sensitivity of the high precision frequency determination can be used to characterize the trap in more detail.

IV. CHARGE TO MASS RATIO DETERMINATION—ACCURACY OF THE METHOD

From the measurement shown in Fig. 2 the *Q/M* ratio has been determined to be +100.9 mC/kg using Eq. (7). This absolute value requires the accurate knowledge of ω, Ω, V_0, and z_0. Although all three eigenfrequencies are determined with high resolution, due to the splitting of the radial fre-

quency and the apparent shift of the frequencies ω_x and ω_z, only ω_y has been chosen for further analysis. The particle is positively charged. This can be checked easily by the polarity of the voltage necessary to lift the particle as being used in the electrodynamical balance.[13,29] Assuming for the moment the particle consisted of one 500 nm SiO_2 particle, the mass is expected to be $M=131$ fg. The corresponding charge of $Q=+1.32\times10^{-17}$ C is equivalent to a net charge of 83 positive elementary charges e. From the majority of measurements, it turns out that most trapped particles carry a few up to several ten positive elementary charges upon storage in the trap. The particle from Fig. 2 carries a comparable large number of charges since it has been subject to charging by the electron gun.

A. Accuracy

As has been pointed out, only ω, Ω, V_0, and z_0 enter the formula to determine Q/M [see Eq. (7)]. Therefore, the accuracy of the determination of Q/M is given by the accuracy of these quantities. While ω and Ω can be determined quite accurately (100 ppm range, ppm range, respectively), the determination of V_0 in the present experiment is good to within a fraction of a percent. The dominant uncertainty is however the absolute determination of the quadrupole parameter z_0. Although the uncertainty due to numerical errors is smaller than one percent, mechanical misalignments or displacements of the electrodes of a few ten μm can relate to errors in the percent range. Therefore, the absolute uncertainty is believed to be about 1%. This lack of knowledge will be overcome in future experiments by calibrating the trap with an atom or molecule of a known charge to mass ratio. A candidate with a high fluorescence rate is a single Ca^+ ion.

Another source of error is related to systematic deviations of the linear relation between the stability parameter, q, and the normalized eigenfrequency, β, for finite q values, i.e., finite adiabaticity. Those deviations have been corrected even for very small q values using the well known formulas relating β and q and a.[1,9] Other uncertainties are again related to the approximations made in the derivation of the key equations. In particular, additional forces, of permanent or alternating nature, seem to be present as has been seen by the splitting of the radial frequency. In the worst case, assuming all frequencies are shifted, errors in the percent range are obviously present. Further calibration measurements should be used to rule out such systematic deviations. In return, one will learn more about the nature of these forces.

V. ABSOLUTE CHARGE STATE AND MASS DETERMINATION

In order to determine the absolute charge state and mass a second independent method for the determination of one of the quantities has to be employed. Various techniques such as Mie scattering[30] or damping by gas friction[16,8] have been used in the past to determine a particles mass. Alternatively, charging, ΔQ, of a particle can be used to determine Q. This requires two frequency measurements, ω_1 at an initial charge state Q, and ω_2 at a charge state $Q+\Delta Q$. As a result, it follows

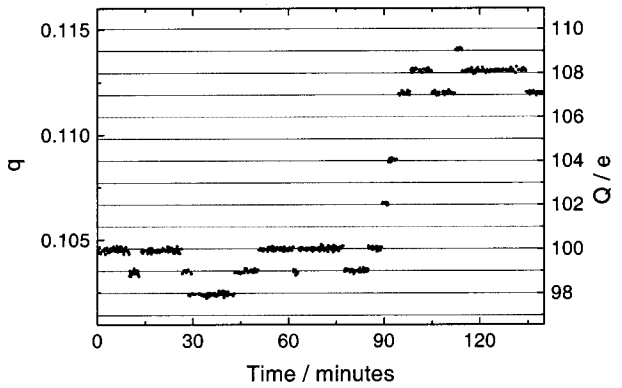

FIG. 4. Step charging of a single 500 nm SiO_2 sphere during the online determination of its eigenfrequency. From this quantity, the stability parameter q, left-hand axis, is derived and displayed here as a function of time. The charging current is so low that collisions occur only every 5 to 10 min. Therefore, the emission of secondary electrons is clearly separated as individual events with $\Delta Q=(n-1)e$, n an integer and e the elementary charge. From $\Delta Q=-e$ events, the absolute number of charges, $Z=Q/e$, is determined, see right-hand axis. The corresponding mass of the particle is $M=1.80\times10^{-16}$ kg.

$$Q=\Delta Q\omega_1/(\omega_2-\omega_1). \tag{11}$$

Using an electron gun to charge a particle at a known charging current density j, the change of charge is then $\Delta Q=j\sigma\Delta t$, where σ is the effective charging cross section of the particle and Δt the charging time. Due to the finite number of elementary charges on the particle (see Sec. IV A) and the high precision of the frequency measurement charging events can be observed as a series of steps in the eigenfrequency. This ''electron stepping'' has been demonstrated by Philip *et al.*[28] on larger particles in an electrodynamical balance by measuring the balancing voltage before and after such a step. An example of such jumps in the present experiment is given in Fig. 4. Here, the charging current is small enough in order to resolve the process as single events. Every primary electron hitting the particle has a chance to stick. For the positively charged particle, this is seen as a sudden decrease in frequency, e.g., the first step in Fig. 4. This corresponds to a charging of $\Delta Q=-e$, where e is the fundamental constant $1.602\ 176\ 462\times10^{-19}$ C. Alternatively, while the primary electron is slowed down on its way into the solid, it may release a number, n, of secondary electrons. This is seen as a sudden increase of the frequency, related to a charging of

$$\Delta Q=+(n-1)e. \tag{12}$$

Note that in this case, it is not necessary to know the charging current but to use the absolute charge state of the particle as a measure. Substituting Eq. (12) in Eq. (11) leads to $Q=(n-1)\omega_1/(\omega_2-\omega_1)e$ and for $n=0$ simply to $Q=\omega_1/(\omega_1-\omega_2)e$. Thus, the charge state is the nearest integer, Z to $(n-1)\omega_1/(\omega_2-\omega_1)$ and $\omega_1/(\omega_1-\omega_2)$, respectively. As a result, in Fig. 4, the corresponding charge state is given as an additional axis. Plugging in the initial charge state of $+100$ e into the initial charge to mass ratio of $Q/M=0.089$ C/kg, it turns out that the particle has a mass of $M=1.80\times10^{-16}$ kg. This mass is larger than expected for a single 500 nm particle (1.3×10^{-16} kg) because in the

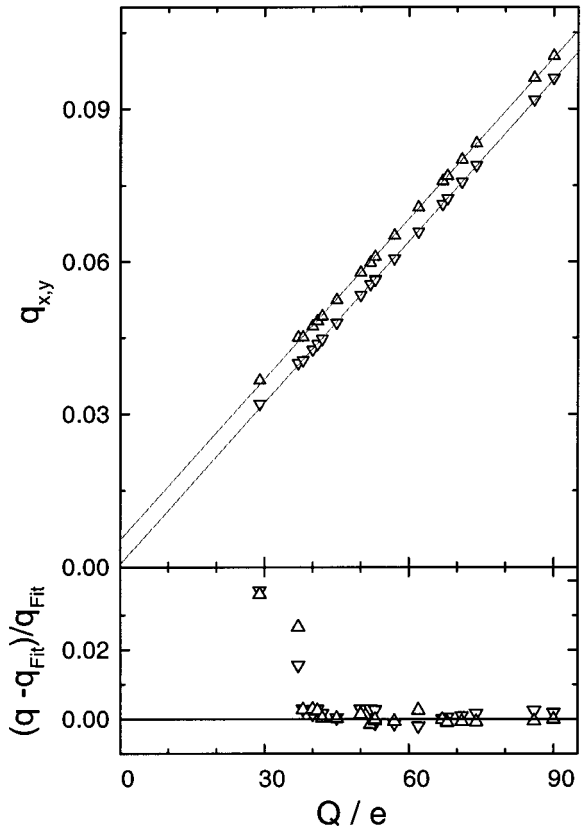

FIG. 5. Linear relationship between stability parameter q_x, q_y and the charge state of a single 500 nm SiO_2 particle. Upper panel: q-values for the horizontal (x direction, $\triangle$) and vertical (y direction, ∇) frequencies have been determined for 18 different charge states of one particle. The charge state of this individual particle is increased by a factor of 3 throughout the experiment. As expected by theory (solid lines), q is strictly proportional to Q [see Eq. (6a) and (6b)]. Lower panel: Deviations from linearity are smaller than 1% for most of the measurements.

present case, C_{60}, from an effusive beam, has been deposited on the particle prior to the charging events seen here.

A. Linearity of the method

During the measurement shown in Fig. 4, the total charge has been changed by about 10%. The resulting charge states coincide quite nicely with the grid of integer multiple elementary charges. This shows that over a small range of Q/M values, the method is linear. Results for the higher charge states ($Q > 105e$) do however not agree as well as the ones for lower charge states. Following Eq.(6a) and (6b), the Q/M value is strictly proportional to q_z and q_r. Due to the limitations in the accuracy discussed, it is worthwhile checking the linearity over a wider range. This has been done by charging one particle from 30 elementary charges up to 90 elementary charges. q values have been determined using the horizontal and the vertical frequencies measured. The $q_{x,y}$ values range from 0.03 up to about 0.1 which is well within the limit of adiabaticity. Both curves are neatly linear over the full range. Moreover, results for both directions follow the same slope as expected. However, due to the splitting of the radial frequency, they are offset by a fixed value in q. The relative deviation, $(q_x - q_y)/(q_x + q_y)$, is however decreasing for increasing Q/M values. As previously described in this article, the vertical frequency, ω_y, has been used for the determination of the absolute charge state, see lower axis. For clarity, deviations from the linearity are given in the lower panel of Fig. 5. For the majority of the measurements, the deviations are well below the 1% range. Larger deviations occur for the lowest charge states. This is due to the need for stronger dc compensation fields which lead to systematic deviations in the eigenfrequency. This influence is diminishing for lighter particles or those with more charge. In summary, the linearity of the experiment is quite striking over a range of factor 3 of the charge state.

VI. CONCLUSIONS—FUTURE APPLICATIONS

In this article, a method for the determination of the absolute mass of charged particles in a three-dimensional quadrupole trap is described. The method is nondestructive due to the optical detection. The instrument has been characterized in various test measurements. They key features of high-resolution (10^4/10 s, 10^5/h), reproducibility, long-term stability (5 ppm/h), accuracy (percent range), and good linearity of the present experimental setup have been quantified.

At present, the particle size which can be investigated is limited by the amount of scattered light being detectable. As a guideline, a power of about 60 fW is scattered in 4π from a 50 nm SiO_2 particle, $M = 1.3 \times 10^{-19}$ kg$\approx 10^8$ u, at illumination conditions presented here. A large fraction of this light can be collected with a trap design as open as the one shown in Fig. 1. In the case of a nonabsorbing particle, of course, higher laser fluences can be employed without disturbances. Therefore, corresponding light levels of more than 10^4 photons per second make this size a safe boundary for scattered light detection. Even this limitation will be overcome by the detection of optical emission from the particle itself, e.g., fluorescence from the particle or from an incorporated chromophore. In the case of a strongly absorbing particle, black body radiation from its surface will become more intense than scattered light. Also, nonlinear detection schemes such as second harmonic generation are possible.[31]

With these technical improvements, a mass range from atomic mass, 1 u, up to picogram, 10^{12} u, can be covered by this technique. For larger masses, eigenfrequencies will be below 1 Hz where this technique becomes less practical. Switching to EDB operation might however be an interesting alternative. The higher mass range is especially interesting because it can be accessed only by the EDB or the method presented here. Additional features of the trapping technique are useful for many experiments. At room temperature, the particle is confined to a volume of a few ten μm cubed. This good localization corresponds to a density of 10^9 cm^{-3} which can be even increased at lower temperatures or with the use of laser cooling or electrical cooling of the particles motion. The storage of a *single* particle can be used in various ways. Since no ensemble averaging effects are present, there is no necessity for the production of uniform particles. In addition, the particles are very well isolated from the environment, e.g., no substrate or other influences.

Many experiments can make use of this interesting instrument. As a precise mass spectrometer, it can be used to

measure the adsorption and desorption of gases as an increase or decrease of the mass of the particle. With its high precision, single atom mass resolution will become feasible. Thus, it will be possible to study surface reactions on the surface of a nanoparticle. For example in astrophysics, the formation of molecular hydrogen on the surface of a dust grain is a long standing problem.[32]

In another surface science experiment, the emission of secondary electrons can be detected. This is the underlying process of the charging events observed in the measurement of Fig. 4. Due to the low charge state of the particle, these measurements make it possible to determine the yields of the secondary electron emission of a quasineutral insulator material. Resolving the jumps in the charge state also provides information about the statistical nature[33] of this process. Results on the yields for a bare SiO_2 particle which is covered *in situ* with C_{60} after the first characterization will be presented elsewhere.[27]

In the past, EDBs have been used quite frequently in the field of aerosols. More detailed studies of the physics and chemistry of the gas/solid (liquid) interface will be possible with this instrument. Further aspects regarding the optical detection can be used to obtain additional information about the particle. The angular distribution of the light scattered contains information about the size, shape, and optical properties, i.e., the refractive index (real and imaginary part), of the particle. Light emission contains similar information. The polarization of light can be used as a further tool.[30] Extending the frequency range, synchrotron radiation might be used for light scattering as well as an ionization source. The absorption of IR radiation will heat the particle resulting in a detectable mass loss which can be sensitive enough to probe thin layers of an adsorbate on its surface.

Other quantities of the particle can be studied if they are the cause for additional forces. A simple example is the gravitational force which is proportional to the particles mass. In the EDB application and also in our setup, this force is compensated by the electrical force acting on the particles charge. Another application deals with the diameter of the particles and the corresponding drag forces.[8] Other forces which can be used for the characterization of the particle are the light scattering and light gradient forces, which can lead to similar or even much larger accelerations as gravity. In case of gradient forces, they can even be used to store a particle.[16] Here, diameter, shape, and refractive index of the particle enter the force. At higher pressures, photophoretic and thermophoretic forces are relevant. Dielectrophoretic forces play an increasing role for larger particles. Here, the mass as well as the refractive index of the particle enter the force. Most of these forces can be utilized by either compensating two forces or by measuring their influence on the eigenfrequency of the particle. In cases when additional forces lead to a more complex motion, additional frequencies will appear in the spectrum.

In summary, this high precision mass spectrometer device can be used in many current fields of science. There are also speculative considerations to use this method as a basis for an alternate definition of the kg. As a scale, the formation of a macroscopic object whose mass is determined to single atom accuracy could be used to link the atomic mass range to micrometer-sized particles. Collecting many such well weighed particles in a second step, a link to the absolute mass unit, might become feasible.[34]

ACKNOWLEDGMENT

This work was supported by the Deutsche Forschungsgemeinschaft in the projects INK2/A3 and the Schwerpunktprogramm SPP 471/SCHL341/2-3.

[1] H. Dawson, *Quadrupole Mass Spectrometer and its Applications* (Elsevier, Amsterdam, 1976).
[2] W. C. Wiley and L. H. McLaren, Rev. Sci. Instrum. **26**, 1150 (1955).
[3] S. M. Michael, B. M. Chien, and D. M. Lubman, Anal. Chem. **65**, 2614 (1993).
[4] A.G. Marshall, C. L. Hendrickson, and G. S. Jackson, Mass Spectrom. Rev. **17**, 1 (1998).
[5] R.F. Wuerker, H. Shelton, and R. V. Langmuir, J. Appl. Phys. **30**, 342 (1959).
[6] W. Paul, Nobel Lecture (1989), E. Fisher, Z. Phys. **156**, 26 (1956).
[7] D. Gerlich, Adv. Chem. Phys. **132**, 1 (1992).
[8] G. Hars and Z. Tass, J. Appl. Phys. **77**, 4245 (1995).
[9] March and Hughes, *Quadrupole Storage Mass Spectrometry* (Wiley, New York, 1989).
[10] *CRC Series in Modern Mass Spectrometry* edited by R. E. March and J. F. J. Todd (1995).
[11] M. H. Friedman, A. L. Yergey, J. E. Campana, J. Phys. E **15**, 53 (1982).
[12] E. C. Beaty, J. Appl. Phys. **61**, 2118 (1987).
[13] S. Arnold, J. Aerosol Sci. **10**, 49 (1979).
[14] N. R. Whetten, J. Vac. Sci. Technol. **11**, 515 (1974).
[15] E. Joos and A. Lindner, Z. Phys. D: At., Mol. Clusters **11**, 295 (1989).
[16] A. Ashkin, Opt. Lett. **11**, 288 (1986).
[17] T. B. Jones, *Electromechanics of Particles* (Cambridge University Press, Cambridge, UK, 1995).
[18] W. Neuhauser, M. Hohenstatt, P. Toschek, and H. Dehmelt, Appl. Phys. (Berlin) **17**, 123 (1978).
[19] J. Illemann, Ph.D. thesis, TU-Chemnitz, 2000; http://archiv.tu-chemnitz.de/pub/2000/0067/.
[20] The driving voltage is applied to the end caps only, one phase operation. For clarity, the formulas given in Sec. II are derived for the more general, symmetrically driven trap, two phase operation. In order to use these general expressions, the amplitude of the voltage applied to the end caps is $2\ V_0$ in the current one phase setup.
[21] SIMION 3D V 6.0, Lockheed Martin Idaho Technologies, 1995.
[22] Mitsubishi Company, model ML419-R.
[23] H. C. van de Hulsst, *Light Scattering by Small Particles* (Dover, New York, 1981).
[24] Hamamatsu Company, model C5460-01.
[25] Merck Company, specific mass $\rho=(2.0\pm0.1)$ g/cm^3. Using electron micrographs, we determined the diameter of the particles to be 498 ± 36 nm (2σ).
[26] P. W. Erdman and E. C. Zipf, Rev. Sci. Instrum. **53**, 225 (1982).
[27] S. Schlemmer, J. Illemann, S. Wellert, and D. Gerlich, J. Appl. Phys. (submitted).
[28] M. A. Philip, F. Gelbard, and S. Arnold, J. Colloid Interface Sci. **91**, 507 (1983).
[29] E. J. Davis, Aerosol. Sci. Technol. **26**, 212 (1997).
[30] B. Krämer, O. Hübner, H. Vortisch, L. Wöste, T. Leisner, M. Schwell, E. Rühl, and H. Baumgärtel, J. Chem. Phys. **111**, 6521 (1999).
[31] E. C. Y. Yan and K. B. Eisenthal, J. Phys. Chem. B **104**, 6686 (2000); J. L. Dadap, J. Shan, K. B. Eisenthal, and T. F. Heinz, Phys. Rev. Lett. **83**, 4045 (1999).
[32] D. Gerlich, J. Illemann, and S. Schlemmer, in *Molecular Hydrogen in Space*, edited by F. Combes and G. Pineau des Forets (Cambridge University Press, Cambridge, UK, 2000).
[33] P. Varga and H. Winter, *Particle Induced Electron Emission II*, Springer Tracts in Modern Physics (Springer, Berlin, 1992).
[34] *Comprehensive Mass Metrology*, edited by M. Kochsiek and M. Gläser (Wiley, New York, 2000).